Linear and nonlinear optical properties of GaAs/AlxGa1−xAs/GaAs/AlyGa1−yAs multi-shell spherical quantum dot

Article *in* Journal of Applied Physics · November 2013

DOI: 10.1063/1.4829703

CITATIONS
30

READS
543

3 authors:

Ahmet Emre Kavruk
Selcuk University
9 PUBLICATIONS **109** CITATIONS
SEE PROFILE

Mehmet Sahin
Abdullah Gul University
58 PUBLICATIONS **1,751** CITATIONS
SEE PROFILE

Fatih Koç
Ahi Evran Üniversitesi
18 PUBLICATIONS **156** CITATIONS
SEE PROFILE

Linear and nonlinear optical properties of GaAs/AlxGa1−xAs/GaAs/AlyGa1−yAs multi-shell spherical quantum dot

Ahmet Emre Kavruk, Mehmet Sahin, and Fatih Koc

Citation: J. Appl. Phys. **114**, 183704 (2013); doi: 10.1063/1.4829703
View online: http://dx.doi.org/10.1063/1.4829703
View Table of Contents: http://jap.aip.org/resource/1/JAPIAU/v114/i18
Published by the AIP Publishing LLC.

Linear and nonlinear optical properties of $GaAs/Al_xGa_{1-x}As/GaAs/Al_yGa_{1-y}As$ multi-shell spherical quantum dot

Ahmet Emre Kavruk,[1,a)] Mehmet Sahin,[1,2,b)] and Fatih Koc[1]
[1]*Physics Department, Faculty of Sciences, Selcuk University, 42075 Konya, Turkey*
[2]*Department of Material Sciences and Nanotechnology Engineering, Abdullah Gul University, Kayseri, Turkey*

(Received 15 August 2013; accepted 24 October 2013; published online 11 November 2013)

In this work, the optical properties of $GaAs/Al_xGa_{1-x}As/GaAs/Al_yGa_{1-y}As$ multi-shell quantum dot heterostructure have been studied as a function of *Al* doping concentrations for cases with and without a hydrogenic donor atom. It has been observed that the absorption coefficient strength and/or resonant absorption wavelength can be adjusted by changing the *Al* content of inner-barrier and/or outer-barrier regions. Besides, it has been shown that the donor atom has an important effect on the control of the electronic and optical properties of the structure. The results have been presented as a function of the *Al* contents of the inner-barrier *x* and outer-barrier *y* regions and probable physical reasons have been discussed. © *2013 AIP Publishing LLC*. [http://dx.doi.org/10.1063/1.4829703]

I. INTRODUCTION

The latest developments in the production technology makes the precise fabrication of low dimensional semiconductor quantum nano structures possible, such as quantum wells, wires, and dots, layer by layer in intended geometry.[1–3] These structures have found a large area of application in many branches of science including chemistry, biology, medicine, engineering, and physics. Such materials draw attention of the researchers thanks to their interesting physical properties. Thus, these structures are widely studied both theoretically and experimentally.[4–10] The electronic and optical properties of quantum dots (QDs) can be tuned by controlling the geometry of the structures, combinations of materials. This controllability and their own unique characteristics provide some advantages to the researchers in fabrication of new generation devices, such as, single electron transistors,[4] QD lasers,[5] single-photon source,[6,7] quantum computing,[11,12] optical memory,[9,13] infrared detectors,[14–16] and QD solar cells.[17–19]

The existence of an impurity in a QD results in interesting physical consequences because of the strong Coulomb interaction between the electron and impurity atom.[2] The impurity in a QD strongly influences the energy levels and corresponding wave functions, the ground level being the most effected.[20,21] Because of this, besides the electronic and optical properties, device performance of the structure can change drastically. Therefore, a hydrogenic donor problem is a very useful model in the understanding of the electronic and optical properties of the QD structures with impurities and many studies related to this subject have been reported.[20–25]

Absorption is the basic physical process in the working of solar cells, infrared photodetectors, and many similar optical devices. Hence, the understanding of the optical absorption in such structures is crucial in the production of new generation hi-tech devices. For example, the energy levels and depending on these, the resonant absorption wavelength can be tuned via size of the QD or combinations of the QD materials. Nonlinear optical properties are as important as the linear ones in the device fabrication. For this reason, both linear and nonlinear optical properties of core/shell QD heterostructures were investigated by many researchers recently.[26–31]

Precise production of multi-shell quantum dot (MSQD) structures has become available with the latest improvements in the lithographic techniques and wet chemical synthesizing methods.[1,3] Many experimental and theoretical studies have been reported about the electronic and optical properties of these structures.[20,21,25] Aktas *et al.* have calculated the energy states and the binding energy of a hydrogenic impurity in a multi-layered spherical GaAs-(Ga, Al)As quantum dot as a function of the barrier thickness and the inner dot thickness for various barrier potentials with and without influence of a magnetic field.[22,23,32] Sahin *et al.* have examined the electronic and linear optical properties of a MSQD with parabolic confinement as a function of layer thicknesses.[24,33] Very recently, Naimi and Jafari have investigated the oscillator strengths, the linear, third-order nonlinear and total absorption coefficients, and refractive index of multi-layered quantum dot and multi-layered quantum anti-dot with a hydrogenic impurity.[34–36] Kostic and Stojanovic[37] have studied influence of the internal heterostructure on nonlinear absorption spectra for intersubband transitions in spherical CdSe/ZnS MSQD nanoparticles. Holovatsky and Frankiv[38] have theoretically investigated the oscillator strength of inter-band transition as functions of the position of hydrogen-like donor impurity in multi-shell spherical QDs.

In this study, the electronic and optical properties of $GaAs/Al_xGa_{1-x}As/GaAs/Al_yGa_{1-y}As$ MSQD heterostructure are thoroughly investigated for cases with and without an on-center donor impurity for different alloy compositions. Schrödinger equation is solved fully numerically in order to determine the electronic structure for different *x* and *y* contents. The transition energies, oscillator strengths, linear, third-order nonlinear, and total absorption coefficients are determined as a function of the *x* and *y* contents by using the obtained energy values and wave functions.

[a)]Electronic mail: aekavruk@selcuk.edu.tr, aekavruk@gmail.com
[b)]Electronic mail: mehmet.sahin@agu.edu.tr, mehsahin@gmail.com

II. DETAILS OF THE CALCULATIONS

A. Model and theory

In this study, we have considered a spherically symmetric MSQD structure as seen in Fig. 1. In the structure, the core radius is R_1, the barrier width is $B_w = R_2 - R_1$, and the well width is $W_w = R_3 - R_2$. In BenDaniel-Duke boundary conditions, the radial Schrödinger equation of the structure is

$$\left[-\frac{\hbar^2}{2}\vec{\nabla}_r\left(\frac{1}{m^*(r)}\vec{\nabla}_r\right) + \frac{\ell(\ell+1)\hbar^2}{2m^*(r)r^2} - \frac{Ze^2}{\kappa(r)r} + V(r)\right]R_{n\ell}(r) = E_{n\ell}R_{n\ell}(r). \tag{1}$$

Here, $\hbar$ is the reduced Planck constant, $m^*(r)$ is the position dependent effective mass, n is the principle quantum number, ℓ is the angular momentum quantum number, Z is the charge of the impurity, $\kappa(r)$ is the position dependent dielectric constant, $V(r)$ is the confinement potential, $R_{n\ell}(r)$ is the radial wave function, and $E_{n\ell}$ are energy levels for the electron. It is noted that $Z=0$ for the case without the impurity and $Z=1$ for the case with the impurity.

The core and well regions contain *GaAs*. The material composition of first barrier region, between R_1 and R_2, is $Al_xGa_{1-x}As$ and of the second one, between R_3 and R_4, is $Al_yGa_{1-y}As$. A schematic representation of the potential profile of the structure is seen in the right panel of Fig. 1. The figure has been plotted for $x=0.15$, $y=0.30$ and $x=0.30$, $y=0.15$. The confinement potential, effective masses, and dielectric constants values, depending on *Al* content, used in the calculations can be found in the literature.[39]

The Schrödinger equation of the system in Eq. (1) was discretized in radial direction and reduced to a numerical matrix diagonalization problem using the finite difference technique. The distance between two-mesh points was 0.001 in units of effective Bohr radius. The ALGLIB subroutine was used to diagonalize the matrix.

B. Linear and non-linear optical properties of the system

The calculations of linear and third-order nonlinear optical properties of the MSQD structure have been carried out using linear, $\chi^{(1)}$, and third-order nonlinear, $\chi^{(3)}$, optical susceptibilities. The analytic forms of $\chi^{(1)}$ and $\chi^{(3)}$ can be obtained for a two-level quantum system as[26,31,40,41]

$$\varepsilon_0\chi^{(1)}(\omega) = \frac{N|M_{ji}|^2}{E_j - E_i - \hbar\omega - i\hbar\Gamma_{ji}}, \tag{2}$$

and

$$\varepsilon_0\chi^{(3)}(\omega) = -\frac{N|M_{ji}|^2|E(\omega)|^2}{E_j - E_i - \hbar\omega - i\hbar\Gamma_{ji}} \times \left[\frac{4|M_{ji}|^2}{(E_j - E_i - \hbar\omega)^2 - i\hbar\Gamma_{ji}} - \frac{(M_{jj} - M_{ii})^2}{(E_j - E_i - i\hbar\Gamma_{ji})(E_j - E_i - \hbar\omega - i\hbar\Gamma_{ji})}\right], \tag{3}$$

where indices i and j correspond to initial and final states, N is the electron density in the MSQD, ε_0 is the dielectric permittivity of the vacuum, Γ_{ji} is the relaxation rate, and $E(\omega)$ is the incident radiation field. E_i and E_j are the initial and final sublevel energies of the MSQD. The energy levels were determined by numerical solution of the radial Schrödinger equation. M_{ji} is the transiton matrix element between the initial and final states. Here, we have chosen z direction for the polarization of the incident light, and hence the transition matrix element is given as

$$M_{ji} = \langle\psi_j|ez|\psi_i\rangle, \tag{4}$$

where ψ_i and ψ_j are the wave functions of the initial and final states. These wave functions are determined by multiplication of the radial wave functions obtained from Eq. (1) with the spherical harmonics, i.e., $\psi_{n\ell m} = R_{n\ell}(r)Y_{\ell m}(\theta,\phi)$. It should be noted that $M_{ii} = M_{jj}$ vanishes in Eq. (3) because of the selection rule, $\Delta\ell = \pm 1$, which follows from the orthogonality of spherical harmonics.

The absorption coefficient is calculated from the susceptibility χ by sing the relation

$$\alpha(\omega) = \omega\sqrt{\frac{\mu}{\varepsilon_r}}\mathrm{Im}(\varepsilon_0\chi(\omega)), \tag{5}$$

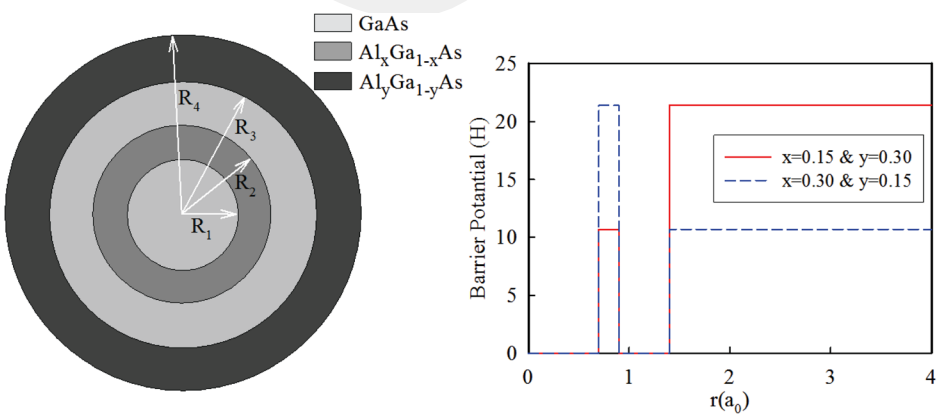

FIG. 1. Schematic representation of the MSQD heterostructure and its potential profile. Red and blue lines correspond to x = 0.15, y = 0.30 and x = 0.30, y = 0.15, respectively, for Al content.

where μ is the permeability of the material and ε_r is the real part of the permittivity of the confinement region. Hence, the linear and third-order absorption coefficients are given as[26,31,40,41]

$$\alpha^{(1)}(\omega) = \omega\sqrt{\frac{\mu}{\varepsilon_r}}\frac{N\hbar\Gamma_{ji}|M_{ji}|^2}{(E_j - E_i - \hbar\omega)^2 + (\hbar\Gamma_{ji})^2}, \tag{6}$$

and

$$\alpha^{(3)}(\omega, I) = -\omega\sqrt{\frac{\mu}{\varepsilon_r}}\left(\frac{I}{2\varepsilon_0 n_r c}\right)\frac{4N\hbar\Gamma_{ji}|M_{ji}|^4}{\left[(E_j - E_i - \hbar\omega)^2 + (\hbar\Gamma_{ji})^2\right]^2}. \tag{7}$$

Here, $n_r = \sqrt{\varepsilon_r}$ is the refractive index of the confinement region and c is the speed of light in the vacuum. The electron density term N is calculated from

$$N = \frac{n}{V_{MSQD}}, \tag{8}$$

where n is the number of electrons in the structure and V_{MSQD} is the volume of the confinement region.

The total absorption coefficient, which is sum of the linear and third-order nonlinear coefficients, is written as

$$\alpha(\omega, I) = \alpha^{(1)}(\omega) + \alpha^{(3)}(\omega, I). \tag{9}$$

The oscillator strength, which is a measure of the optical transition, is a unitless and an important quantity in understanding of the optical phenomena. It is calculated by means of

$$O_{ji} = \frac{2m^*}{\hbar^2}(E_j - E_i)|M_{ji}|^2. \tag{10}$$

III. RESULTS AND DISCUSSION

Throughout the calculations, we have used atomic units in which charge, bare mass of the electron and Planck constant are taken to be unity, i.e., $m_0 = e = \hbar = 1$. In these units, the effective Bohr radius is $1a_0 = 0.529\frac{\kappa}{m^*} \cong 100$ Å and the effective Rydberg energy is $1R_y = 13.6\frac{m^*}{\kappa^2} \cong 5.25$ meV, corresponding to the material parameters of GaAs. The effective mass of GaAs is $m_{GaAs} = 0.067m_0$ and the dielectric constant is $\kappa_{GaAs} = 13.18$. The speed of light in the vacuum $c = 3 \times 10^8$ m/s, the permeability of the material is taken as $4\pi 10^{-7}$N/A^2, and $\hbar\Gamma_{ij}$ is taken as 6.4 meV. BenDaniel-Duke boundary conditions have been used at all layer boundaries as follows:

$$\begin{aligned}
\frac{1}{m_1}\frac{dR_{n\ell}(r)}{dr}\bigg|_{r=R_1^-} &= \frac{1}{m_2}\frac{dR_{n\ell}(r)}{dr}\bigg|_{r=R_1^+} \\
\frac{1}{m_2}\frac{dR_{n\ell}(r)}{dr}\bigg|_{r=R_2^-} &= \frac{1}{m_3}\frac{dR_{n\ell}(r)}{dr}\bigg|_{r=R_2^+} \\
\frac{1}{m_3}\frac{dR_{n\ell}(r)}{dr}\bigg|_{r=R_3^-} &= \frac{1}{m_4}\frac{dR_{n\ell}(r)}{dr}\bigg|_{r=R_3^+}.
\end{aligned} \tag{11}$$

The core radius is $R_1 = 0.7\,a_0$ and the other layer thicknesses are chosen as $B_w = 0.2\,a_0$ and $W_w = 0.5\,a_0$. The shell thickness is chosen to allow the tunneling of the electron between the core and well regions. The effective masses m_2 and m_4 in first and second shells, respectively, vary depending on *Al* content.[39]

Figure 2 shows the probability amplitude and energy levels of the MSQD heterostructure for different confinement potentials of shell regions for $Z = 0$ and $Z = 1$ cases. Focusing on the energy states, one can clearly see the effect of the impurity on both ground and excited energy levels, but the effect on the ground states is stronger as expected. Hence, the probability densities of ground states are more confined in the core region because of the attractive Coulomb potential of the impurity atom. Considering the left panel of the figure, we see that while ground states are confined in the core region, the excited ones are confined in the well region with increasing inner-barrier height. This behaviour is more pronounced for $Z = 1$ cases. Namely, separation of the charge densities of ground and excited states becomes more apparent with increasing x. Considering the right panel of the figure, the probability amplitudes of both ground and excited states are pushed from well region to the core with increasing y. This behaviour is more apparent for $1s$ level for $Z = 0$ case. In addition, the energy separation between ground and excited levels increases with increasing y as expected. We conclude that while an increase in the inner-barrier potential height results in the separation of probability amplitudes, the increase in the outer-barrier height increases the separation of the energy levels.

Figure 3 shows the transition energies as a function of x and y for $Z = 0$ (top panel) and $Z = 1$ (bottom panel) cases.

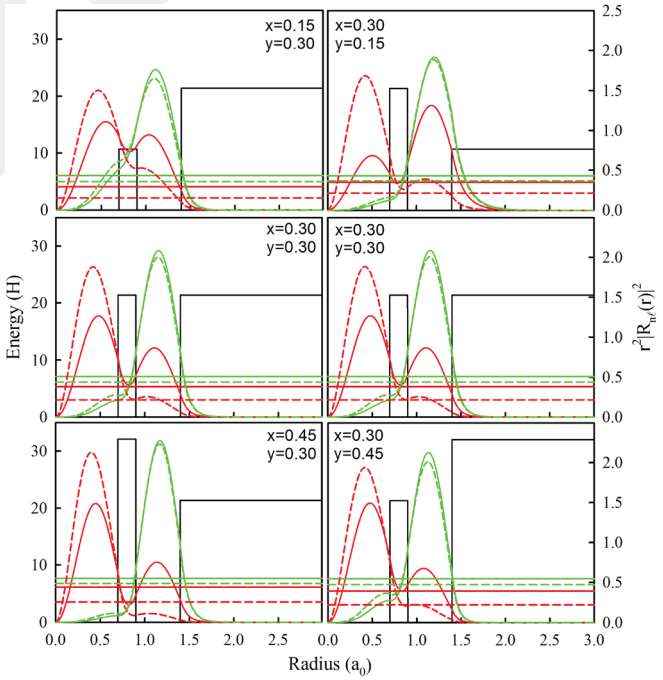

FIG. 2. The electronic structure of MSQD heterostructure. The red and green lines show $1s$ and $1p$ states, respectively while black lines correspond to potential profile of the structure. The solid and dashed lines correspond to $Z = 0$ and $Z = 1$ cases, respectively. The straight lines indicate the energy levels.

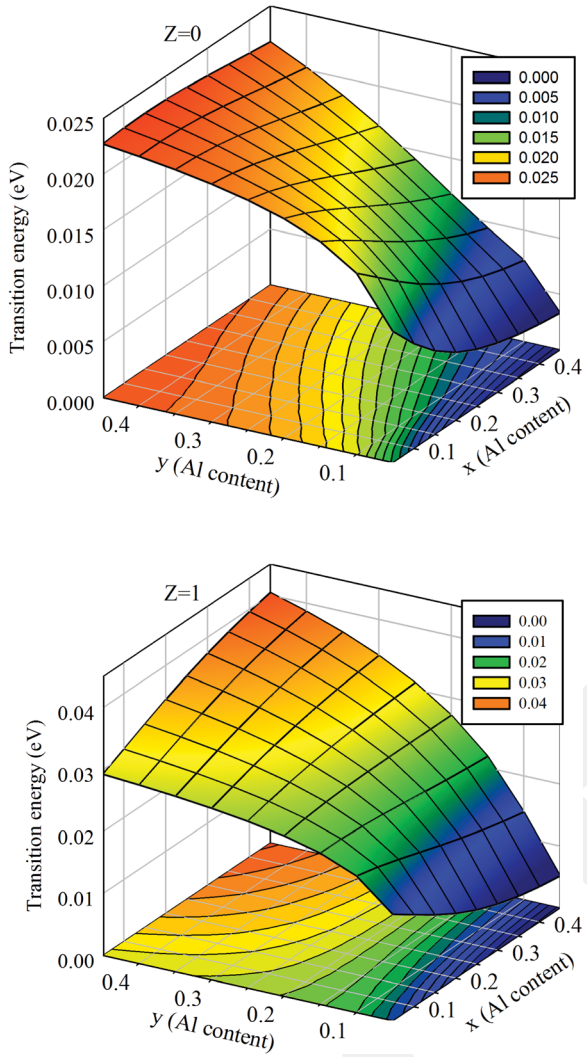

FIG. 3. The transition energies as a function of the x and y contents, top panel for $Z=0$ case and bottom panel for $Z=1$ case.

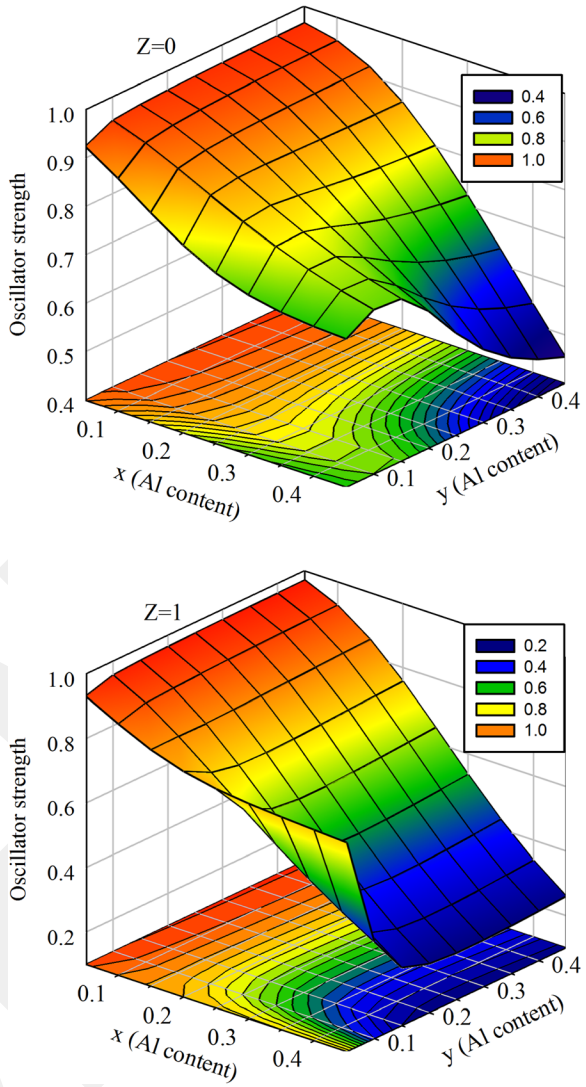

FIG. 4. The inter-sublevel oscillator strength of the MSQD heterostructure as a function of x and y contents for $R_1=0.7$, $B_w=0.2$, and $W_w=0.5\,a_0$.

When we compare the two panels, we see that the transition energies of $Z=0$ case are smaller than those of the $Z=1$ case. Changes in x do not strongly effect the transition energies, however its effect is more pronounced for the case with impurity. On the other hand, changes in the y content is more effective on the transition energies for both $Z=0$ and $Z=1$ cases. The increasing of y content results in a stronger overall confinement and therefore a blue shift is observed in the transition energies. The existence of the impurity hinders the tunneling in to the shell region and thus pronounces the effect of the x content.

The oscillator strength, a unitless quantity, provides important information about the transition probabilities; and therefore, it is a very important parameter for analysing the optical properties of a quantum structure. As can be seen from Eq. (10), the oscillator strength is directly related to the transition energies and overlap integral of the wave functions of ground and excited states. The oscillator strength as a function of the x and y contents are presented in Fig. 4 for $Z=0$ (top panel) and $Z=1$ (bottom panel) cases. When we look at the figures, we observe that the variation of oscillator strength strongly depends on the x content for both cases. The oscillator strength is almost independent of y for small x values, while there is a strong dependence on y for larger x values. The oscillator strengths for $Z=0$ and $Z=1$ cases show distinctly different behaviour. For $Z=0$, electrons can easily tunnel through the barrier for smaller x values and the transition matrix element and thus oscillator strength has large values approaching to unity. However, for larger x values tunneling is hindered and only resonant tunneling is allowed thus the oscillator strength shows a maximum for some value of y. On the other hand, for $Z=1$ case, the tunneling is suppressed by the Coulomb interaction and the oscillator strength is small for almost all y values. For very small values of y, the excited state becomes unconfined and probably this results in the rapid increase observed in calculated oscillator strengths.

The linear, third-order nonlinear, and total absorption coefficients have been plotted in Figure 5 for different x and y contents. On the left panel, y is taken as 0.3; and similarly on the right panel, the x is fixed to 0.3. Generally, we observe that the linear and third-order nonlinear absorption coefficients of $Z=0$ cases are larger in comparison with

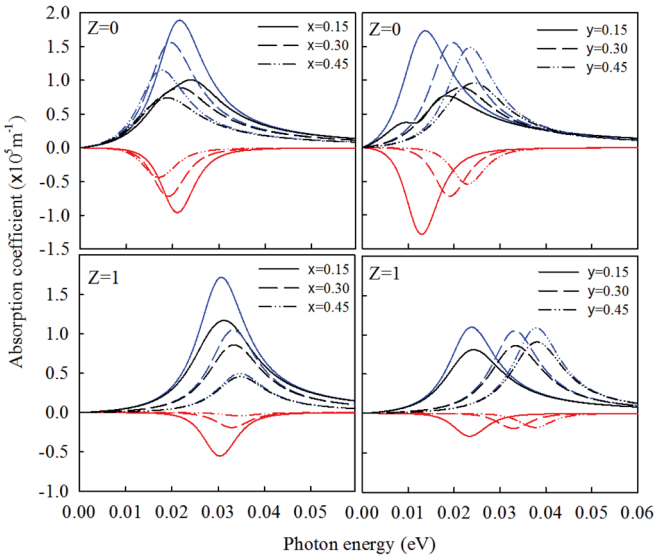

FIG. 5. Linear (blue lines), third-order nonlinear (red lines), and total (black lines) absorption coefficients as a function of the photon energy for different x (left panel) and y (right panel) values. The photon intensity is taken as $0.4\,MW/cm^2$. Top and bottom panels show the cases of $Z=0$ and $Z=1$, respectively.

those of $Z=1$, which should be expected because the impurity suppresses the tunnelling which in turn results in smaller transition matrix elements and smaller absorption coefficients. In addition, when we compare the top and bottom panels, we see that the absorption peak energies, corresponding the energy difference between the initial and final states, move to higher energies for $Z=1$ cases for all x and y values. When we look at the left panel of the figure, all absorption coefficients decrease significantly with increasing x content. This is because the overlapping decreases with increasing x values. If we focus on the right panel of the figure, although there are no drastic changes in the absorption coefficients, the absorption peak energies shift towards higher energies (blue-shift) with increasing y values. These controllable properties can be very useful to tune the sensitivity or working wavelength of the opto-electronic devices such as quantum dot infrared photodetectors.

IV. CONCLUSION

We have carried out a detailed investigation of the electronic and optical properties of $GaAs/Al_xGa_{1-x}As/GaAs/Al_yGa_{1-y}As$ multi-shell QD heterostructure as a function of x and y contents for cases with and without the impurity. We have shown that magnitude of the absorption coefficient or the absorption wavelength or both of them can be tuned by adjusting x and y contents in MSQD. These properties are especially important for device fabrication such as quantum dot infrared photodetectors or other optoelectronic devices. In addition, we observe that the impurity has important influence on the electronic structure, which in turn strongly affects the linear and nonlinear optical properties of the structure. We hope that this study contributes to understanding of electronic and optical properties of MSQD heterostructures and stimulates new experimental studies related to device applications.

ACKNOWLEDGMENTS

This work was partially supported by Selcuk University BAP office. One of the authors (M. S.) thanks Abdullah Gul University Foundation for their support. The authors thank U. Atav for illuminative discussions.

[1]D. Bimberg, M. Grundmann, and N. N. Ledentsov, *Quantum Dot Heterostructures* (Wiley, Chichester, 1999).
[2]P. Harrison, *Quantum Wells, Wires and Dots: Theoretical and Computational Physics*, 3rd ed. (John Wiley, Chippenham, Great Britain, 2009).
[3]V. I. Klimov, *Nanocrystal Quantum Dots*, 2nd ed. (CRC Press, Taylor and Francis Group, LLC, 2010).
[4]E. Leobandung, L. Guo, and S. Y. Chou, Appl. Phys. Lett. **67**, 2338 (1995).
[5]N. Kristaedter, O. G. Schmidt, N. N. Ledentsov, D. Bimberg, V. M. Ustinov, A. Yu. Egorov, A. E. Zhukov, M. V. Maximov, P. S. Kopev, and Zh. I. Alferov, Appl. Phys. Lett. **69**, 1226 (1996).
[6]P. Michler, A. Kiraz, C. Becher, W. V. Schoenfeld, P. M. Petroff, L. Zhang, E. Hu, and A. Imamoglu, Science **290**, 2282 (2000).
[7]O. Benson, C. Santori, M. Pelton, and Y. Yamamoto, Phys. Rev. Lett. **84**, 2513 (2000).
[8]V. Bondarenko and Y. Zhao, J. Phys.: Condens. Matter **15**, 1377 (2003).
[9]M. Kroutvar, Y. Ducommun, D. Heiss, M. Bichler, D. Schuh, G. Abstreiter, and J. J. Finley, Nature **432**, 81 (2004).
[10]S. A. Nasrallah, A. Bouazra, A. Pnocet, and M. Said, Physica E **43**, 146 (2010).
[11]K. K. Likharev, IBM J. Res. Dev. **32**, 144 (1988).
[12]D. Loss and D. P. Divicenzo, Phys. Rev. A **57**, 120 (1998).
[13]K. Imamura, Y. Sugiyama, Y. Nakata, S. Muto, and N. Yokoyama, Jpn. J. Appl. Phys., Part 2 **34**, L1445 (1995).
[14]S. Kim, H. Mohseni, M. Erdtmann, E. Michel, C. Jelen, and M. Razeghi, Appl. Phys. Lett. **73**, 963 (1998).
[15]S. Maimon, E. Finkman, G. Bahir, S. E. Schacham, J. M. Garcia, and P. M. Petroff, Appl. Phys. Lett. **73**, 2003 (1998).
[16]X. Jiang, S. S. Li, and M. Z. Tidrow, Physica E **5**, 27 (1999).
[17]J. Wu, D. Shao, Z. Li, M. O. Manasreh, V. P. Kunets, Z. M. Wang, and G. J. Salamo, Appl. Phys. Lett. **95**, 071908 (2009).
[18]J. Wu, S. Lee, V. R. Reddy, M. O. Manasreh, B. D. Weaver, M. K. Yakes, C. S. Furrow, V. P. Kunets, M. Benamara, and G. J. Salamo, Mater. Lett. **65**, 3605 (2011).
[19]J. Wu, Y. F. M. Makableh, R. Vasan, M. O. Manasreh, B. Liang, C. J. Reyner, and D. L. Huffaker, Appl. Phys. Lett. **100**, 051907 (2012).
[20]M. Sahin, F. Tek, and A. Erdinc, J. Appl. Phys. **111**, 084317 (2012).
[21]H. Taş and M. Sahin, J. Appl. Phys. **111**, 083702 (2012).
[22]S. Aktas and F. K. Boz, Physica E **40**, 753 (2008).
[23]F. K. Boz, S. Aktas, A. Bilekkaya, and S. E. Okan, Appl. Surf. Sci. **255**, 6561 (2009).
[24]M. Sahin and K. Köksal, Semicond. Sci. Technol. **27**, 125011 (2012).
[25]H. Taş and M. Sahin, J. Appl. Phys. **112**, 053717 (2012).
[26]M. Sahin, J. Appl. Phys. **106**, 063710 (2009).
[27]S. Nizamoglu and H. V. Demir, Opt. Express **16**, 3515 (2008).
[28]S. Yilmaz and H. Safak, Int. J. Mod. Phys. B **23**, 2127 (2009).
[29]B. Çakir, Y. Yakar, A. Özmen, M. Ö. Sezer, and M. Şahin, Superlatt. Microstruct. **47**, 556 (2010).
[30]A. Özmen, Y. Yakar, B. Çakir, and Ü. Atav, Opt. Commun. **282**, 3999 (2009).
[31]W. Xie, Phys. Lett. A **372**, 5498 (2008).
[32]F. K. Boz, S. Aktas, A. Bilekkaya, and S. E. Okan, Appl. Surf. Sci. **256**, 3832 (2010).
[33]S. Akgül, M. Sahin, and K. Köksal, J. Lumin. **132**, 1705 (2012).
[34]Y. Naimi and A. R. Jafari, J. Comput. Electron. **11**, 414 (2012).
[35]A. R. Jafari and Y. Naimi, J. Comput. Electron. **12**, 36 (2013).
[36]A. R. Jafari, Y. Naimi, and S. Davatolhagh, Opt. Quantum Electron. **45**, 517 (2013).
[37]R. Kostic and D. Stojanovic, Phys. Scr. **T149**, 014055 (2012).
[38]V. A. Holovatsky and I. B. Frankiv, J. Optoelectron. Adv. Mater. **15**, 88 (2013).
[39]S. Adachi, J. Appl. Phys. **58**, R1 (1985).
[40]C.-H. Liu and B.-R. Xu, Phys. Lett. A **372**, 888 (2008).
[41]J. Yuan, W. Xie, and L. He, Physica E **41**, 779 (2009).